ISIJ International, Vol. 51 (2011), No. 12, pp. 1967–1973

Atmosphere Controlled Hot Thermocouple Method and Crystallization Phenomenon of $CaO–Al_2O_3$ Eutectic Slag

Yoshiaki KASHIWAYA,[1)] Yasuaki KUSADA[2)] and Ryosuke O. SUZUKI[3)]

1) Graduate School of Energy Science and Technology, Kyoto University. Yoshida Honmachi, Sakyoku, Kyoto, 606-8501 Japan. 2) Formerly Graduate Student, Graduate School of Eng., Hokkaido University. Now at Nippon Steel Corporation, Ohita Works, Nishi-no-su, Ohita, 870-0992 Japan. 3) Graduate School of Eng., Faculty of Engineering, Hokkaido University, Kita-13Jou, Nishi-8Choume, Kita-ku, Sapporo, Hokkaido, 060-8628 Japan.

(*Received on May 6, 2011; accepted on July 19, 2011*)

A desulfurization slag is difficult to recycle, since there is a possibility to elute a sulfur containing solution. To promote the recycle of the desulfurization slags, it is important to know the physicochemical properties of the slag. In addition, desulfurization process could be modified, when the sulfur behavior in the slag was understood.

In this study, the effect of sulfur and oxygen partial pressure on the crystallization behavior was investigated using Hot Thermocouple Technique. Three different atmospheres were established in the electric furnace through the modification of experimental apparatus. One was an argon without deoxidation, the second was an argon with Ti plate (Ar+Ti) which was located in the electric furnace for deoxidation of argon gas, and the third was an argon with CaS pellet located on the Ti plate (Ar+Ti+CaS) in which the partial pressure of SO_2 increased with the decrease of the oxygen partial pressure.

The nose position of TTT diagram of $CaO–Al_2O_3$ eutectic composition under Ar atmosphere was 7 s at 1 100°C, while the nose positions under Ar+Ti and Ar+Ti+CaS were 7 s at 1 150°C. TTT diagrams under Ar+Ti and Ar+Ti+CaS, which are lower oxygen potential and higher SO_2 potential, showed the earlier crystallization behavior in the higher temperature region than the nose position. From the results of XRD analysis, the sulfur added to the slag existed in the monocalcium aluminate ($CaO·Al_2O_3$) primary crystal. When the content of CaS increased, a formation of CaO through oxidation increased and the tricalcium aluminate ($3CaO·Al_2O_3$) was formed as a primary crystal, in which the sulfur content was higher than the eutectic structure in the matrix.

KEY WORDS: TTT diagram; desulfurization slag; hot thermocouple; crystallization.

1. Introducton

The steelmaking industry, which is one of important field sustaining the base of the society, is facing a severe situation from securing the resources and decreasing the CO_2 emission. Saving the energy and resources is the biggest problem and the countermeasures are conducted with the utmost effort. Although, the amount of CO_2 emission from Japanese steelmaking industry is lowest (http://www.jisf.or.jp/, (at Mar. 2011)), the absolute amount of CO_2 emission is large because of the huge production of iron. Therefore, the influence on the reduction of CO_2 can be large on the total reduction of CO_2 emission and it is the effective way carrying out on the iron and steelmaking field.

Among the countermeasures for saving the resources and energy, a recycle and reuse of slags are one of the effective ways, because slags contain many kinds of elements and have a high temperature around 1 500°C, when it is exhausted. There are many kinds of slags depending on the purpose which makes the recycle of slags difficult.

Particularly, a desulfurization slag is difficult to use for a landfilling or roadbed material, because there is a possibility to discharge a sulfur containing eluate from slag. To promote the recycle of the desulfurization slags, it is important to know the physicochemical properties of the slag. In this study, the effect of sulfur on the crystallization behavior was investigated using Hot Thermocouple Technique.[1–3)] When the physicochemical properties of a sulfur containing slag are examined, it is important to decrease the oxygen potential for preventing the oxidation of sulfur in the slag. The experimental system was modified for decreasing the oxygen potential using titanium plate closely located to the sample melt. Furthermore, CaS pellet was used to fix the partial pressure of SO_2 in the atmosphere. The TTT diagram of $CaO–Al_2O_3$ system was measured using Single Hot Thermocouple Technique (SHTT).

2. Experimental

2.1. Experimental Apparatus with the Sulfur Potential Controlled

Figure 1 shows the experimental apparatus including the hot thermocouple (HT) driver and the observation system consisted of CCD camera, which are able to control through

a personal computer. A small electric furnace (alumina tube; 10 mmϕ I.D, 12 mmϕ O.D, 20 mmL) with platinum heater (0.5 mmϕ), which is to minimize the temperature gradient in the sample melt on the hot thermocouple, was located at the center of quartz tube.

The details of hot thermocouple method are summarized in the previous papers.[1,2)]

One of the purposes of the present study is to clarify the behavior of sulfur in slag during solidification and the reaction with the oxygen in the atmosphere. The reaction between CaS in slag and oxygen in gas phase can be expressed by Eq. (1).

$$\text{CaS (in slag)}+3/2\text{O}_2\text{ (g)} = \text{CaO (in slag)} + \text{SO}_2\text{ (g)} \quad ..(1)$$

CaS will react with oxygen and form CaO. The rate of reaction is quite fast, if the oxygen partial pressure is high. **Figure 2** shows the TPP (temperature-partial-pressure, or phase stability) diagram of Ca–O–S system,[4)] when the activities of CaS and CaO are unity or almost the same and the oxygen partial pressure P_{O_2} equals to 10^{-15}Pa (9.869×10^{-21}atm). $CaSO_4$ is stable below 584°C, the equilibrium partial pressure of SO_2 changes from 0.026 ($\log P_{SO_2}$=–1.59Pa at 584°C) to 3.98×10^{-17} ($\log P_{SO_2}$= –16.4 at 300°C). On the other hand, CaS is stable more than 584°C, when the equilibrium partial pressure of SO_2 decreases from 0.026 ($\log P_{SO_2}$=–1.59Pa at 584°C) to 3.98×10^{-11} ($\log P_{SO_2}$=–10.4Pa at 1 000°C).

The content of oxygen in Ar used was about 5 ppm which meant that the oxidation of CaS occurred easily. In this study, deoxidation by a titanium metal was performed to be CaS in slag stable. The equilibrium partial pressure of oxygen through the oxidation of titanium, P_{O_2} is estimate as 10^{-15}Pa at 1 405°C (Eq. (2)).[4)] Although many kinds of titanium oxides existed in a low oxygen pressure region between TiO_2 and Ti, it was difficult to determine the phase of Ti oxide. A representative oxygen partial pressure was calculated using the equilibrium between TiO_2 and Ti.

$$\text{Ti}+\text{O}_2=\text{TiO}_2 \quad P_{O_2}=10^{-15}\text{Pa, T=1 405°C} \quad ..... (2)$$

The broken line in Fig. 2 shows the equilibrium line between TiOx (TiO_2, Ti_6O_{11}, Ti_5O_9, Ti_3O_5, Ti_2O_3, TiO) and TiS_x (TiS_3, TiS_2, TiS).[4)] As the partial pressure of SO_2 on the TiO_x–TiS_x equilibrium is higher than that of CaO–CaS equilibrium, CaS equilibrium region exists without a formation of TiS_x (**Fig. A-1**),[4)] when a partial pressure of oxygen P_{O_2} equals to 10^{-15}Pa. If P_{SO_2} was very high, TiSx would form simultaneously. However, since the actual P_{SO_2} will control by CaO–CaS equilibrium, titanium sulfides does not form on the titanium plate. Actually, XRD analysis was performed after several experiment and any titanium sulfide did not detected.

If the temperature of titanium was below 1 405°C, the equilibrium oxygen partial pressure, P_{O_2} could be less than 10^{-15}Pa and the stable area of CaS could be expanded. Oppositely, when the P_{O_2} increases, the stable area of CaS decreases as shown in **Fig. 3**.[4)]

Figure 4 illustrates the small electric furnace for reducing the heat loss from the sample on the hot thermocouple.

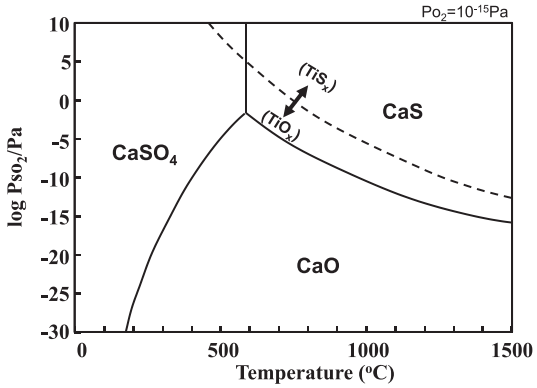

Fig. 2. Ca–O–S system TPP diagram.($Po_2=10^{-15}$Pa, The broken line means the equilibrium line between titanium oxides and sulfides. Cf. Fig. A-1 in appendix).

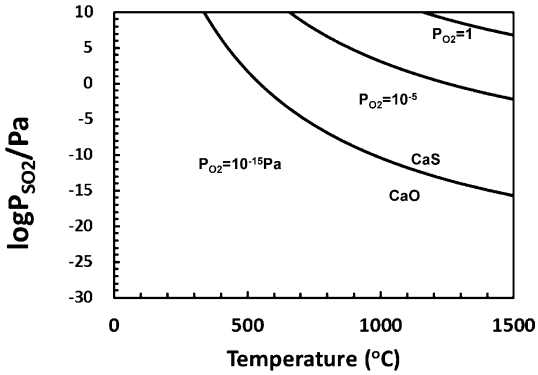

Fig. 3. Equilibrium lines between CaO and CaS when the partial pressures of oxygen are **10^{-15}Pa**, **10^{-5}Pa**, **1.0Pa**.

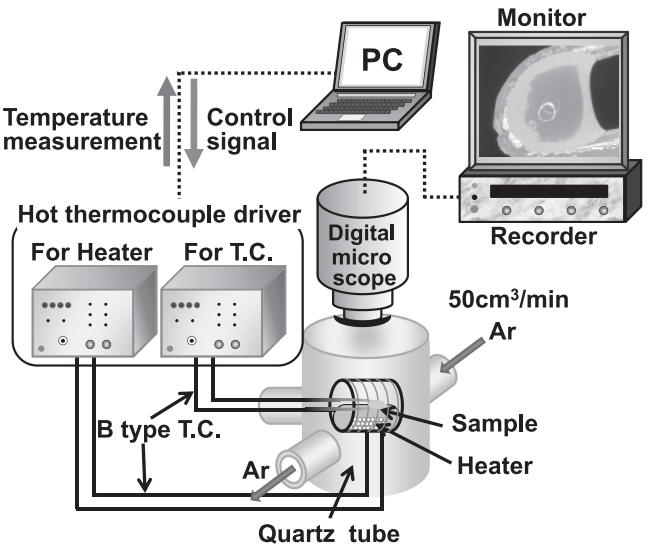

Fig. 1. Schematics of experimental apparatus.

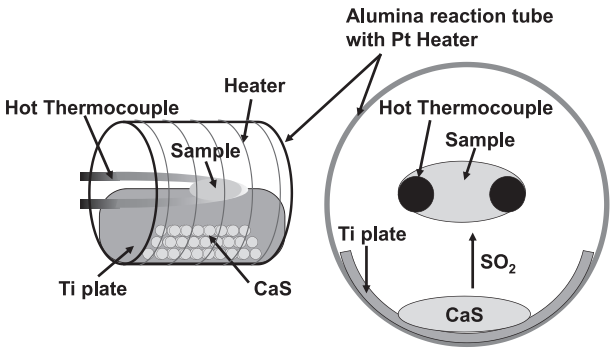

Fig. 4. Electric furnace for reducing the heat loss from sample.

Since the partial pressure of oxygen in the furnace should be maintained as low as possible, the titanium plate for deoxidation is set in the bottom of the electric furnace. Furthermore, in this experiment, a reagent CaS pellet was put on the Ti plate. The reason of the setting CaS pellet was to increase the SO_2 partial pressure for stabilizing the S (in slag), because the oxidation reaction (Eq. (1)) of CaS in the slag was very fast and it was difficult to maintain the sulfur content. When the oxygen partial pressure around sample was still high (even if the titanium plate was used), the reaction between CaS (reagent) and O_2 could form the SO_2 gas which could make the sulfur in the slag stable.

2.2. Slag Sample Served and Atmosphere

The slag sample was prepared in $CaO–Al_2O_3$ binary system (**Fig. 5**).[5–7] The composition at eutectic point is 35.8 mol%Al_2O_3 and the temperature is 1 350°C. A reagent CaO was heated at 1 000°C for 24 hours. After the moisture and hydrate were removed, the CaO was mixed with a reagent α-Al_2O_3. A large amount of the mother slag of CaO–35.8 mol%Al_2O_3 was made and a mixing of CaS was carried out using the same mother slag.

In this study, the composition of mother slag was selected at eutectic point and it was expressed as CA_{EU} for convenience. The CaS additions to the mother slag were 1 mass%, 5 mass% and 10 mass%, which were expressed as CA_{EU}-S1, CA_{EU}-S5 and CA_{EU}-S10 , respectively. The sulfur contents in the slag were 0.35 mol%S, 1.75 mol%S, 3.55 mol%S, respectively. Those compositions are summarized in **Table 1**. In addition, an atmosphere was controlled using a titanium plate and CaS pellet on the titanium plate. The differences of atmosphere were denoted by Ar, Ar–Ti and Ar–Ti–CaS (Table 1).

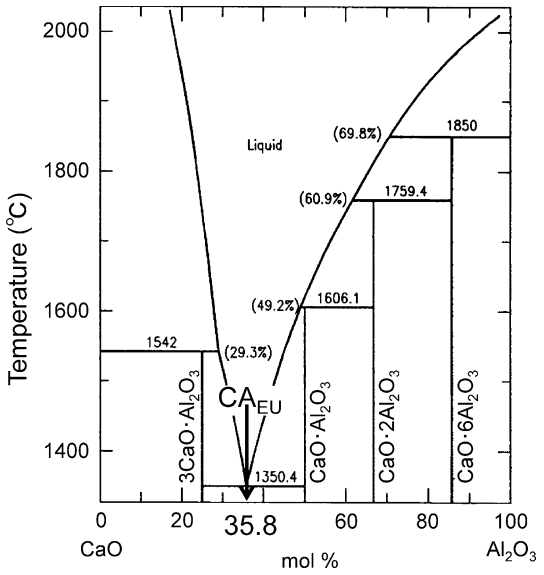

Fig. 5. Phase diagram of $CaO–Al_2O_3$ system.

In this study, the effects of atmosphere on the crystallization phenomenon and TTT diagram of $CaO–Al_2O_3$ eutectic slag were mainly studied. In addition, a CaS was directly added to the CA_{EU}, and the sulfur distribution was examined by EPMA and XRD. However, the effect of sulfur content on TTT diagram will be published in another paper.

3. Results and Discussions

3.1. Crystallization Behavior of Mother Slag (CA_{EU})

Figure 6 shows the melting and crystallizing process of CA_{EU} slag under Ar atmosphere (without Ti). Before experiment, an enough waiting time was taken for the substitution with argon gas. A pressed sample powder about 10 mg was put on the thermocouple, and then the thermocouple was quickly heated up to 1 600°C within 1 minute as shown in Fig. 6. After the melt was stabilized at 1 600°C until a uniform transparent one was obtained, it was quenched to a given temperature (1 300°C) and time was measured for starting and ending crystallization. The starting time of crystallization was about 2 000 s from the quenching. A small opaque crystal was growing from the left edge of sample melt. After 2 005 s, a grew crystal was about 0.5 mm in diameter and the crystallization was finished at 2 015 s, so that the sample became totally opaque.

Using a titanium plate, an oxygen partial pressure in the atmosphere decreased as mentioned above. **Figures 7** and **8** show the results of crystallization at 1 305°C and 1 170°C under Ar–Ti, respectively. At 1 305°C, a crystal phase started to grow from 220 s at the right edge of sample as shown in Fig. 7(a). In this case, the sample melt was translucent a little, which was different from Fig. 6, The direction of crystal grow and the front border of crystal were indicated by a thick arrow and broken line in the Fig. 7. It is difficult to distinguish the position of crystal on the photo, the crystal growing behavior can be understand by the original movie, in addition, the round reflection mark on the surface of sample is changed by the existence of crystal as shown by Figs. 7(a) to 7(d). Comparing with the result in Ar atmosphere (Fig. 6), starting of crystallization was quit early but the growing rate was slow (under Ar (Fig. 6): starting; 2 000 s, ending; 2 015 s, Ar+Ti (Fig. 7): starting; 220 s, ending; 270 s), which meant that the upper line of TTT diagram for the sample under Ar+Ti was moved toward the high temperature region. However, the crystal growing mode resembled each other.

Figure 8 shows the result of observation at 1 170°C under Ar+Ti. The crystal in this condition was changed to a transparent one. Only the difference of an index of refraction can show the existence of crystal regions, however, the trans-

Table 1. Composition of sample slag used and atmosphere.

	CaO mol% (mass%)	Al_2O_3 mol% (mass%)	CaS mol% (mass%)	S mol% (mass%)	Atmosphere		
					Ar	Ar–Ti	Ar–Ti–CaS
CA_{EU}	64.2 (49.7)	35.8 (50.3)	0.00	0.00	○	○	○
CA_{EU}-S1	63.6 (49.2)	35.4 (49.8)	1.00 (1.00)	0.35 (0.44)	○	–	–
CA_{EU}-S5	61.0 (47.2)	34.0 (47.8)	5.02 (5.00)	1.75 (2.22)	○	–	–
CA_{EU}-S10	57.8 (44.7)	32.2 (45.3)	10.0 (10.0)	3.55 (4.44)	○	–	–

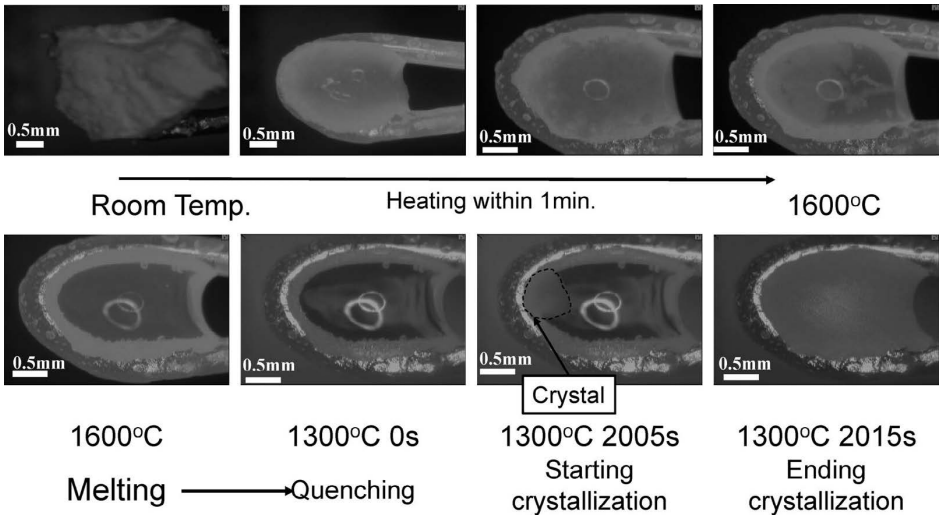

Fig. 6. Melting and crystallizing process of mother slag (CA_{EU}) on the HT under Ar atmosphere (0.5ϕ B type T.C.).

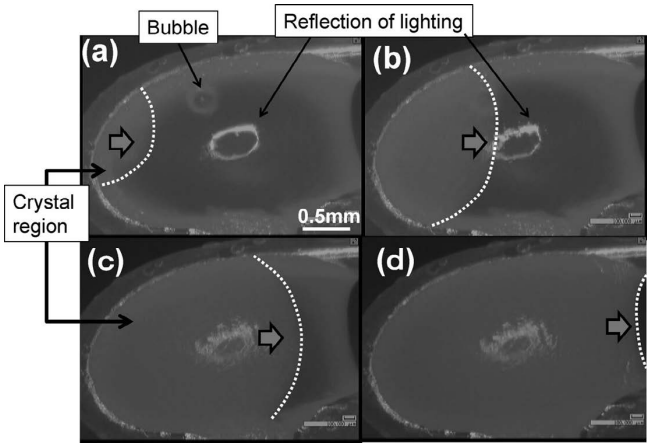

Fig. 7. Crystallization behavior of CA_{EU} under Ar–Ti at 1 305°C. (a) 220 s, opaque crystals, (b) 230 s, opaque crystals, (c) 250 s, opaque crystals, (d) 270 s, opaque crystals.

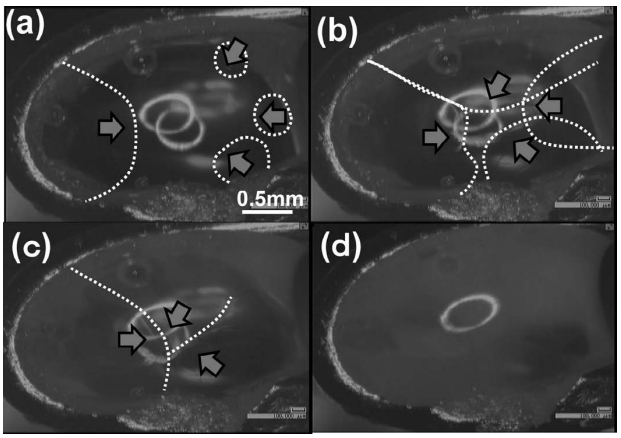

Fig. 8. Crystallization behavior of CA_{EU} under Ar–Ti at 1 170°C. (a) 9 s, transparent crystals, (b) 30 s, translucent crystals, (c) 60 s, translucent crystals, (d) 120 s, opaque crystals.

parent crystal is very difficult to see in the figure. In this case, the crystals started to grow at 9 s from quenching, and grew from 4 different positions as shown by arrows in Fig. 8(a). The early starting time of crystallization from quenching means that it is near to the nose position of TTT diagram. From 60 s (Fig. 8(c)), the crystal began to be translucent and finally it became opaque at 120 s (Fig. 8(d)). The crystallization behaviors in $CaO–Al_2O_3$ system were quite complicated and different from conditions such as the partial pressure of oxygen, temperature and impurities. Especially, the effects of impurity are not known completely. For example, Nurse *et al.*[5,7] have concluded that the compound $Ca_{12}Al_{14}O_{33}(C_{12}A_7)$ is actually a hydrate, $Ca_{12}Al_{14}O_{32}(OH)_2$, and there is no $C_{12}A_7$ compound in $CaO\text{-}Al_2O_3$ system. Although $C_{12}A_7$ was not found in the present study, the effect of low partial pressure of oxygen on the crystal phase of $CaO–Al_2O_3$ system might exist. In addition, Jeevaratnam *et al.*[8] discussed about the effect of two reactive O^{2-} ions in CA system, and the ions would be affected by the oxygen partial pressure in the atmosphere. Accordingly, crystallization behavior of CA system will be affected by the condition of low oxygen potential in the atmosphere.

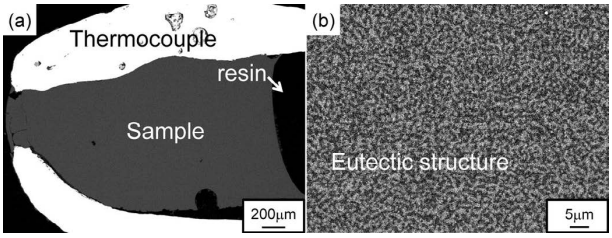

Fig. 9. SEM images of CA_{EU} under Ar at 1 300°C.

Figure 9 shows the result of SEM observation of CA_{EU} at 1 300°C under Ar atmosphere. The sample was completely crystallized at 1 300°C and quenched. Figure 9(a) is a macroscopic image, which is a horizontal plane including the thermocouple portion, and Fig. 9(b) is a microscopic image of the sample. The sample showed a homogeneous structure and was an eutectic microstructure of $CaO–Al_2O_3$ system. From the results of EPMA analysis, the dark area was Al rich and white area was Ca rich, and they were corresponding to monocalcium aluminate ($CaO{\cdot}Al_2O_3$: CA) and tricalcium aluminate ($3CaO{\cdot}Al_2O_3$: C_3A), respectively.

Figure 10 shows a comparison of XRD patterns between the crystallized sample quenched from 1 300°C and the amorphous sample quenched from liquid phase. The quenching system in the present experiment shows an enough cooling speed for getting the amorphous phase. On the other hand, it

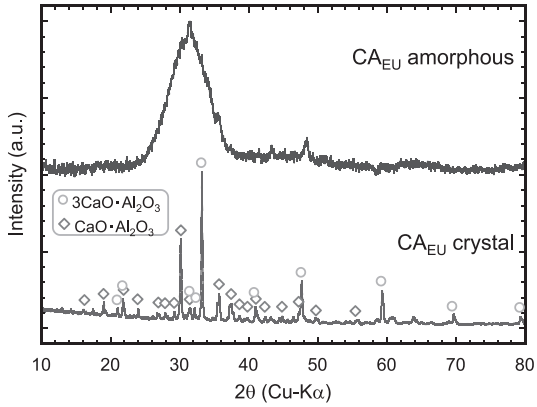

Fig. 10. Comparison of XRD patterns of crystalized phases (CA+C3A) and amorphous phase under Ar.

was confirmed that the crystallized phases consisted of CA and C_3A which was agreed with the result of EPMA analysis.

Figure 11 shows the result of SEM observation of CA_{EU} crystallized under Ar–Ti atmosphere at 1 300°C. Figure 11(a) is a vertical plane cutting at the center of sample including the tip of thermocouple. The plate-like primary crystals of CA were precipitated in the whole sample and the matrix structure was eutectic one. The thickness of CA plate is about 5 μm and the eutectic structure (Fig. 11(b)) in the matrix is coarser than that in Ar atmosphere (Fig. 9(b)). This structure was clearly affected by the low oxygen potential resulted from Ti plate set in the electric furnace. The explanation of this result needs a thermodynamic consideration, however, there is no thermodynamic data on the effect of P_{O_2} for CaO–Al_2O_3 phase diagram.

Figure 12 shows the microstructure of CA_{EU} crystallized at 1 300°C under Ar–Ti–CaS atmosphere. Figure 12(a) shows the cross section of sample in the vertical section including the tip of thermocouple. The CA crystals having a quite interesting morphology were precipitated in the lower part of sample where the surface was near the CaS pellet on the Ti plate. A line analysis by EPMA was performed at the position shown in Fig. 12(a). The result of line analysis is shown in **Fig. 13**. The concentrations of CaO and Al_2O_3 at the matrix are about 66.7 mol% and 33.3 mol%, respectively, which are corresponding to the CA–C_3A eutectic structure. On the other hand, the concentrations of CaO and Al_2O_3 at the dark crystals precipitated are about 50 mol% for both compounds, which corresponds to the CA crystal. In this case, sulfur content was very low and it was difficult to analyze or detect the sulfur in the sample. However, two position showing high sulfur content from 0.03 to 0.058 mol% were found, where was indicated by the arrows. The positions having higher sulfur content were the crystal of CA, however, it was difficult to conclude because the width of crystal was very thin. In the later section XRD analyses were performed to make clear the effect of sulfur contend on the size of unit cell. The detailed discussions were carried out in the later section.

The sulfur was clearly coming from CaS pellet putting on the Ti plate. Overall reaction can be considered as follows. In the CaS pellet:

$$CaS\ (\text{in pellet}) + 3/2O_2\ (g) \rightarrow CaO\ (\text{in pellet}) + SO_2\ (g) \quad \ldots\ldots (3)$$

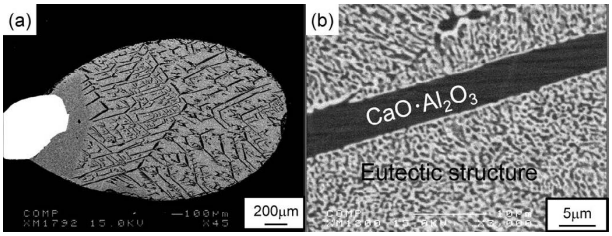

Fig. 11. SEM images of CA_{EU} under Ar–Ti at 1 300°C.

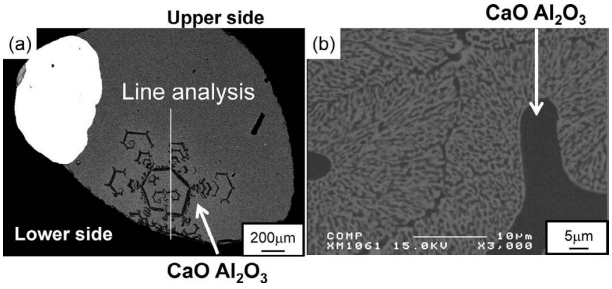

Fig. 12. SEM images of CA_{EU} under Ar–Ti–CaS at 1 300°C.

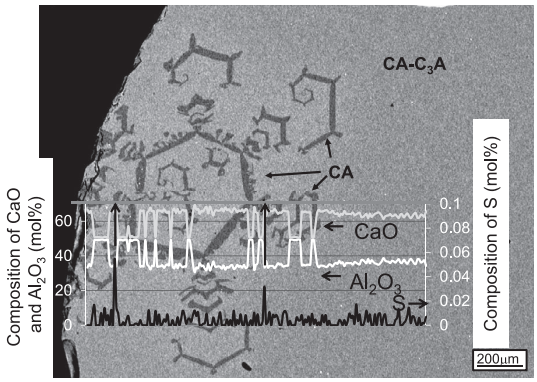

Fig. 13. Line analysis and SEM image of CA_{EU} under Ar–Ti–CaS at 1 300°C.

In the sample melt:

$$SO_2\ (g) \rightarrow S\ (\text{in slag or at surface}) + 2O\ (\text{in slag or at surface}) \quad \ldots\ldots (4)$$

$$CaO\ (\text{in slag}) + S\ (\text{in slag}) \rightarrow CaS\ (\text{in slag}) + O\ (\text{in slag}) \quad \ldots\ldots (5)$$

$$CaS\ (\text{in slag}) + 3O\ (\text{in slag or at surface}) \rightarrow CaO\ (\text{in slag}) + SO_2\ (g) \quad \ldots\ldots (6)$$

The initial sulfur should result from Eq. (3). After SO_2 (g) was absorbed in the slag melt (Eq. (4)), the reaction path cannot be known. However, the exchange reaction between CaO and CaS must exist depending on the balance of oxygen partial pressure and sulfur partial pressure as shown by Eqs. (5) and (6). Furthermore, newly formed CaO (in slag) shown in Eq. (6) might make a nucleation site of CA, which caused the growth of a primary crystal of CA. In the another paper,[10] we distinguished the CaO in Eq. (6) from originally existing CaO and expressed as a CaO*. The effects of sulfur on the solidification of CA slag was discussed.

3.2. TTT Diagrams under Different Atmospheres

TTT diagrams of CA_{EU} under different atmospheres (Ar,

Ar–Ti and Ar–Ti–CaS) were obtained using same technique as shown in the previous studies.[1–3,9] **Figure 14** shows the TTT diagram of CA_{EU} under Ar atmosphere. The solid circles and line means the start of the crystallization, and the solid triangles and line means the end of crystallization. The nose position located at 7 s and 1 100°C. In the high temperature region from the nose position, the time between the start and the end was very short, which meant the growth rate of crystals was high, while in the lower temperature region below the nose position, the growth rate was low. **Figure 15** shows the TTT diagram under Ar–Ti atmosphere. In the case of lower partial pressure of oxygen, the nose position was moved to the high temperature region (1 150°C), but the start time was almost the same (7 s). The line of starting crystallization also moved toward the high temperature region which meant the lower growth rate of crystal in comparison with Ar atmosphere. **Figure 16** shows the TTT diagram under Ar–Ti–CaS atmosphere, which is resemble to the TTT under Ar–Ti atmosphere. This sample was not added the sulfur (CaS) directly, however, a small quantity of sulfur was originated from the gas phase as mentioned above. Since the small content of sulfur existed in the slag, a significant change of TTT diagram was not found. In the another paper,[10] the CaS up to 10 mass% was added directly to the CA_{EU} slag, and the changes of TTT diagrams were discussed.

Figure 17 shows the comparison of the TTT diagram (start of crystallization) among three different atmospheres (Ar, Ar–Ti and Ar–Ti–CaS). The start of crystallization in the lower temperature region below the nose position was almost the same among three conditions, while in the high temperature region, the crystallization in the Ar+Ti and Ar+Ti+CaS atmospheres started earlier than that of Ar atmosphere, for example, about 80 s to 20 s at 1 250°C and about 2 000 s to 200 s at 1 300°C. From the results of SEM observation (Figs. 11 and 12), the formation of primary crystal of CA might related to this phenomenon caused by the lower oxygen partial pressure and the existence of sulfur.

Since the sulfur content of sample under Ar–Ti–CaS was very low, it was difficult to discuss the effect of sulfur in details. The position of sulfur is not known exactly, for example, whether the sulfur exists in the crystals (CA or C_3A) or segregates in the grain boundary or in the eutectic structure. 1 mass%, 5 mass% and 10 mass% of CaS (Table 1) were added to the mother slag (CA_{EU}) and crystallization behaviors were measured under Ar. After quenching from 1 300°C, the samples were examined by XRD. The peak position of (123) of CA ($(123)_{CA}$) and (440) of C_3A ($(440)_{C3A}$) were compared in **Figs. 18** and **19**, respectively. Furthermore, interplanar spaces were calculated and plotted in **Fig. 20**. It was found that the interplanar spaces linearly increased with the increase of sulfur content. From these results, some of sulfur added existed in both of the structure of CA and C_3A. In Fig. 13, the existence of sulfur was found in the position of CA primary crystal, which was agreed with the results of XRD. In addition, when the content of CaS increased, the amount of CaO increased and the formation of compound $3CaO{\cdot}Al_2O_3$ (C_3A) increased through Eq. (6) (the details of result will be published).[10] In this case, the sulfur also existed in the crystal structure of C_3A. However, it was considered that a little amount of sulfur dis-

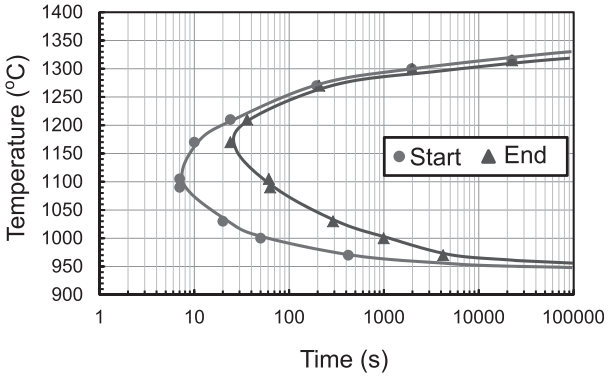

Fig. 14. TTT diagram of CA_{EU} under Ar.

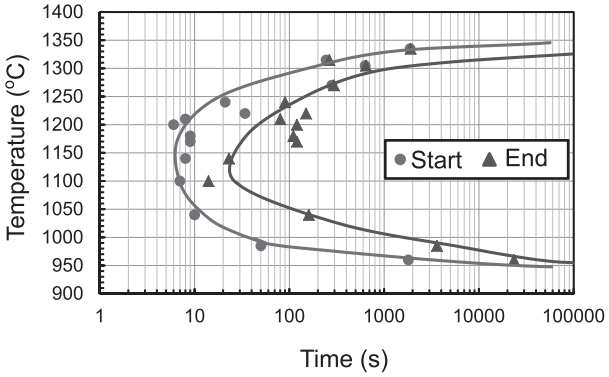

Fig. 15. TTT diagram of CA_{EU} under Ar–Ti.

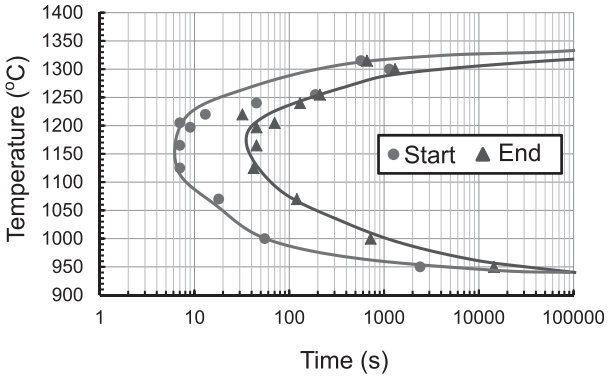

Fig. 16. TTT diagram of CA_{EU} under Ar–Ti–CaS.

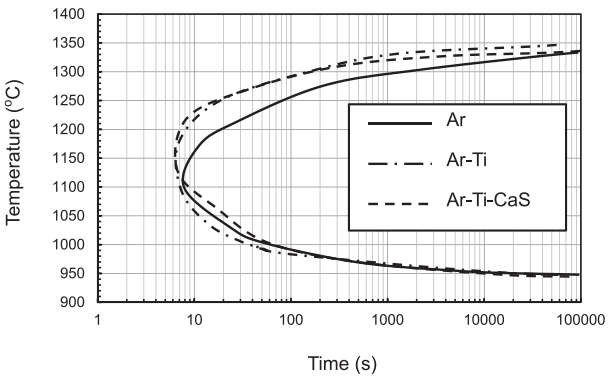

Fig. 17. Comparison of TTT diagrams of CA_{EU} under different atmospheres.

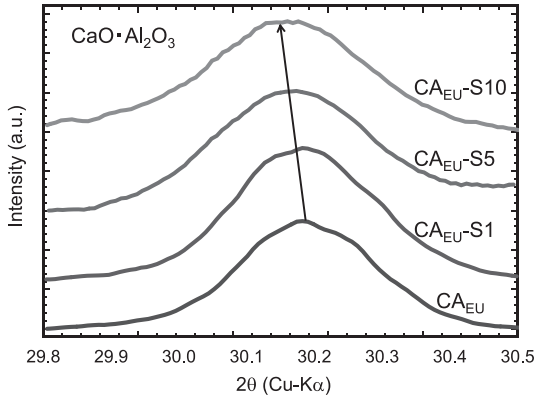

Fig. 18. Shift of (123) peak position of CA with sulfur content.

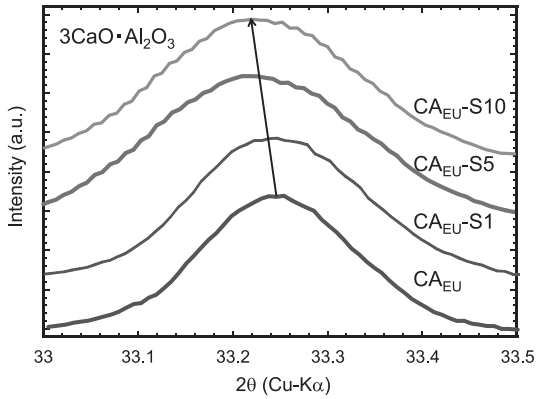

Fig. 19. Shift of (440) peak of C_3A with sulfur content.

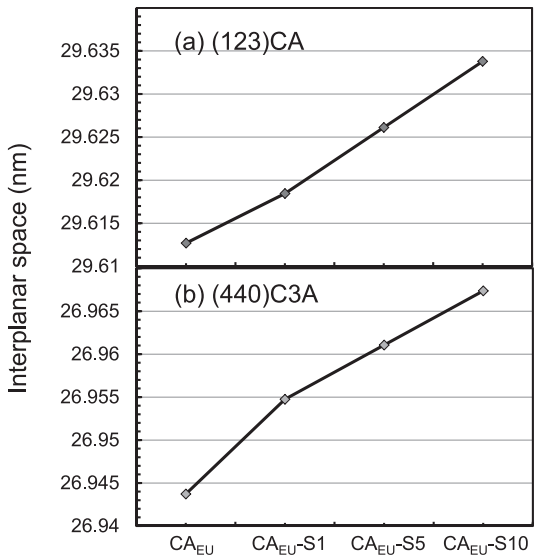

Fig. 20. Variations of Interplanar spacing with sulfur content.

solved in the eutectic structure in the matrix.

4. Conclusions

Using hot thermocouple method, TTT diagrams under three different atmospheres [Ar, Ar+Ti (Ar deoxidized by Ti) and Ar+Ti+CaS (Ar deoxidized by Ti and increased the SO_2 partial pressure)] were measured. Effect of atmosphere on the TTT diagram of $CaO–Al_2O_3$ system was clarified. The microstructure and sulfur distribution were measured by SEM and EPMA. The obtained results are as Follows.

(1) To make the sulfur stable in $CaO–Al_2O_3$–(CaS) slag, it is effective to use the Ti plate and CaS pellet in the furnace owing to decrease P_{O_2} and increase P_{SO_2} in gas phase.

(2) The nose position of TTT diagram under Ar atmosphere was 7 s at 1 100°C, while the nose positions under Ar+Ti and Ar+Ti+CaS was 7 s at 1 150°C.

(3) TTT diagrams under Ar+Ti and Ar+Ti+CaS, which are lower oxygen potential and higher SO_2 potential, showed the earlier crystallization behavior in the higher temperature region than the nose position. The primary crystal was monocalcium aluminate ($CaO·Al_2O_3$: CA) in the both atmosphere, while only eutectic structure was observed under Ar atmosphere, which was relatively high oxygen potential in the gas.

(4) From the results of XRD analysis, the sulfur added to the mother slag (CA_{EU}) existed in the CA primary crystal. When the content of CaS increased, a formation of CaO through oxidation increased and the tricalcium aluminate ($3CaO·Al_2O_3$: C_3A) was formed as a primary crystal, in which the sulfur content was higher than the eutectic structure in the matrix.

REFERENCES

1) Y. Kashiwaya, C. E. Cicutti, A. W. Cramb and K. Ishii: *ISIJ Int.*, **38** (1998), 348.
2) Y. Kashiwaya, C. E. Cicutti and A. W. Cramb: *ISIJ Int.*, **38** (1998), 357.
3) P. Kahn Son and Y. Kashiwaya: *ISIJ Int.*, **48** (2008) 1165.
4) HSC Chemistry for Windows Ver.5.1, Outotec Research Oy. Finland (2002).
5) B. R. W. Nurse, J. H. Welch and A. J. Majumdar: *Trans. Br. Ceram. Soc.*, **64** (1965), 409.
6) A. K. Chatterjee and G. I. Zhmoidin: *J. Mater. Sci.*, **7** (1972), 93.
7) G. Eriksson and A. D. Pelton: *Metall. Trans. B*, **24B** (1993), 807.
8) J. Jeevaratnam, F. P. Glasser and L. S. Dent Glasser: *J. Amer. Soc.*, **42** (1964), 105.
9) Y. Kashiwaya, T. Nakauchi, P. Khanh Son, S. Akiyama and K. Ishii: *ISIJ Int.*, **47** (2007), 44.
10) Y. Kashiwaya, Y. Kusada and R. O. Suzuki: *ISIJ Int.*, **51** (2011) No. 12, 1974.

Appendix

Figure A-1 shows the TPP diagram of Ti–O–S system at $P_{O_2}=10^{-15}$Pa.[4)]

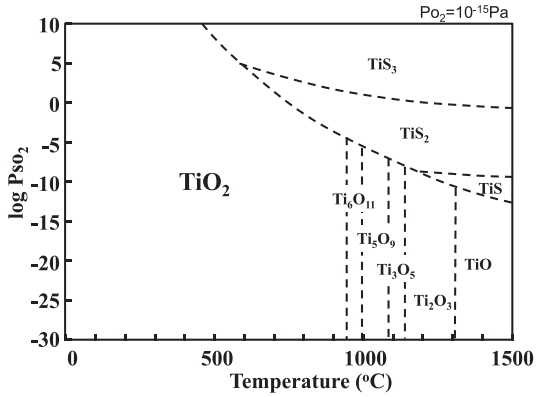

Fig. A-1. Ti–O–S system TPP diagram ($Po_2=10^{-15}$).